Laser-Induced Gas Vortices

Uri Steinitz,[*] Yehiam Prior, and Ilya Sh. Averbukh

Department of Chemical Physics, Weizmann Institute of Science, 234 Herzl Street, Rehovot, Israel 76100
(Received 13 February 2012; revised manuscript received 25 May 2012; published 20 July 2012)

Recently, several femtosecond-laser techniques have demonstrated molecular excitation to high rotational states with a preferred sense of rotation. We consider collisional relaxation in a dense gas of such unidirectionally rotating molecules, and suggest that due to angular momentum conservation, collisions lead to the generation of macroscopic vortex gas flows. This argument is supported using the Direct Simulation Monte Carlo method, followed by a computational gas-dynamic analysis.

Nowadays, femtosecond lasers are routinely used to manipulate and control molecular rotation and orientation in space [1,2]. Particularly, diverse techniques have been developed to bring gas molecules to a rapidly spinning state with a preferred sense of rotation. These schemes include the optical centrifuge [3–5] and the molecular propeller [6,7] methods, excitation by a chiral pulse train [8] and other techniques that are currently discussed [9,10]. In rarefied gas, coherent effects such as alignment revivals have been widely investigated. Most recently, the optical centrifuge method was applied to excite molecules to rotational levels with angular momentum of hundreds of $\hbar$ in dense gas samples [5], where collisions play an important role. In this Letter we analyze the behavior of a dense gas of unidirectionally spinning molecules after many collisions have occurred. The statistical mechanics and equilibration process of such a system are not trivial, as is known for other ensembles in which angular momentum (AM) is a conserved quantity in addition to energy [11,12]. We show that due to the AM conservation, the collisions in such a gas transform the laser induced molecular rotation into macroscopic vortex flows. The lifetime of the generated vortex motion exceeds the typical collision time by orders of magnitude, and the emerging velocity field eventually converges to a self-similar Taylor vortex [13]. The viscous decay of this whirl can be overcome by repeated laser excitations that produce a continuous stirring effect.

Consider a gas sample excited by laser pulses causing the molecules to rotate, on average, unidirectionally. When two rotating molecules collide, the scattering specifics are defined by the random impact details. Due to the momentum conservation law, the linear momenta of the colliding molecules are always equal but opposite in the center-of-mass frame (even for rotationally inelastic collisions). In that frame, the linear momenta are generally noncollinear (cf. Fig 1), thus providing a 'lever arm' for the couple of the linear momentum vectors. We may define the orbital angular momentum, $L = r_{12} \times P$, where r_{12} and $\pm P$ are the intermolecular distance and the linear momenta of the molecules, respectively. The total (conserved) AM of the molecular pair in the center-of-mass frame is the vectorial sum $L_{\text{tot}} = L + J_1 + J_2$, where $J_{1,2}$ represent the individual molecules' internal rotational AM. If initially the molecules rapidly rotate in the same sense, the most probable outcome of the collision is the reduction of the rotational energy, leading to the increase of $|P|$ and a corresponding increase of the orbital AM, L, at the expense of the rotational AM, $J_1 + J_2$. Such collisional transfer of the AM initially stored in the unidirectionally rotating molecules provides a microscopic mechanism for the emergence of the vorticity in the gas flow. As the molecular ensemble approaches equilibrium, the direction of the individual rotational AM is randomized by the collisions and the average rotational AM vector $\langle J_n \rangle$ reduces to zero, thus transferring the AM to the translational motion. This argumentation is rather general and holds irrespective of the details of the interaction potential.

Our analysis of the gas dynamics was performed in two steps. We investigated the initial stages of the transformation of the molecular rotation into collective gas motion with the help of the Direct Simulation Monte Carlo
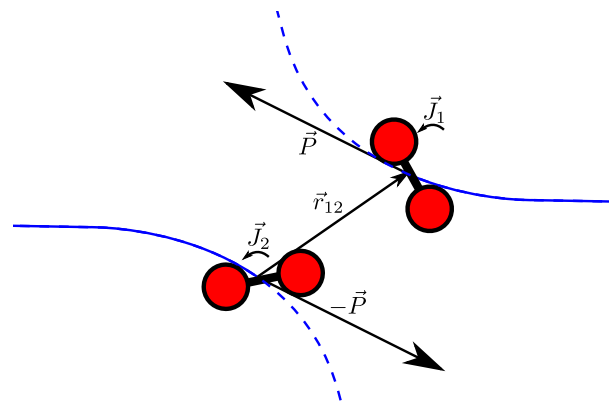

FIG. 1 (color online). Illustration of a sample collision of two rotating molecules in the frame of their center of mass. The loss of the rotational angular momentum, $J_1 + J_2$, is compensated by an increase of the orbital AM, $r_{12} \times P$, due to total AM conservation. The curved arrows illustrate the molecular rotational motion.

(DSMC) technique [14]). Then, after the motion had taken a collective character, we used continuum hydrodynamic equations to investigate the gas dynamics and vortex flow evolution.

The statistical DSMC method is a proven tool for computational molecular dynamics of transitional regimes [15], although the standard DSMC method does not always conserve AM [16,17]. For this reason, we designed an advanced variant of the DSMC simulation in which angular momentum is strictly conserved. The simulation was run in axisymmetric geometry, and handled collisions using a simple 'hard dumbbell' model that treats each "molecule" as a couple of rigidly connected hard spheres [18]. In recent experiments, laser excitation of unidirectional rotation induced an average axial AM in the range of $\langle J_z \rangle \sim 10\hbar$–$400\hbar$ [4,7]. We first simulated a homogeneous sample of such unidirectionally rotating nitrogen molecules put at atmospheric conditions and confined to a smooth cylinder. Figure 2 shows that within about ten collisions (0.3–1.0 ns at our simulation conditions) the energy partition between the translational and rotational degrees of freedom approaches equilibrium. Despite the simplicity of our collision model, it provides the expected energy partition ratio of 3:2 (translation:rotation) typical for diatomic molecules. In the considered example, the molecules completely lose memory of the preferred direction of their rotation by the end of the equilibration period (see the curve for the mean value of the axial molecular AM component in Fig. 2).

At longer times, the confined gas rotates rigidly (with tangential velocity linear with the radius) as seen in Fig. 3. In order to reduce the statistical fluctuations of the Monte Carlo simulation we averaged the results over multiple runs [19]. The rigid-body-like rotation represents a steady state for the motion within a frictionless cylinder, eliminating shear stress. The gas at that stage is in thermal equilibrium, with a small nonvanishing mean value of molecular tangential velocity. This velocity bias, shown in Fig. 3, is about 3 orders of magnitude smaller than the molecular thermal speed. As expected, the results show that the rotation speed is proportional to the total initially induced AM, predicting a steady macroscopic gas rotation frequency of $\sim 10^4$ Hz for initial unidirectional rotation of $\langle J_z \rangle \sim 100\hbar$ at atmospheric conditions within a 10 μm diameter capillary.

At the next stage we analyzed the formation of an unconfined vortex. For this we considered excitation by an axisymmetric laser beam with a Gaussian radial profile. We examined the spatial and temporal development of the circular flow structure around the beam's axis by first running the DSMC simulation for the nonuniform initial rotational excitation. We then sampled and averaged the results of many runs, collecting data corresponding to times following the thermalization stage. We used the processed data as initial conditions for a continuum gas-dynamic analysis that unfolded the subsequent gas behavior. This approach (DSMC followed by computational fluid dynamic simulation) is similar to one that has been used in the past for analysis of the laser-gas interaction [20]. The gas-dynamic equations we used relate to the mass, energy, and momentum conservation in a compressible gas [21]. In order to better account for compressibility we added bulk viscosity [22] terms to the equations, and the ideal gas
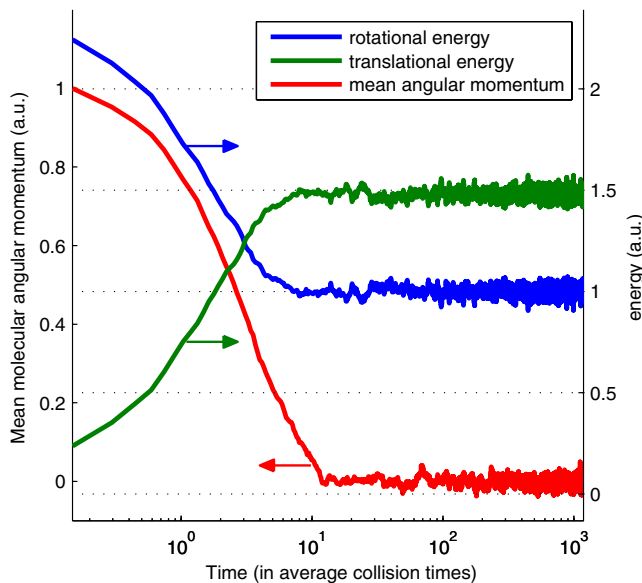

FIG. 2 (color online). Mean translational energy, rotational energy, and molecular axial rotational angular momentum evolution. Initially all the molecules were unidirectionally rotating. The DSMC results show that the final translational:rotational energy ratio reaches 3:2 (green:blue curves, right axis) within about 5–10 collision times. The time axis is logarithmic in units of average collision time ($\sim 10^{-10}$ s).
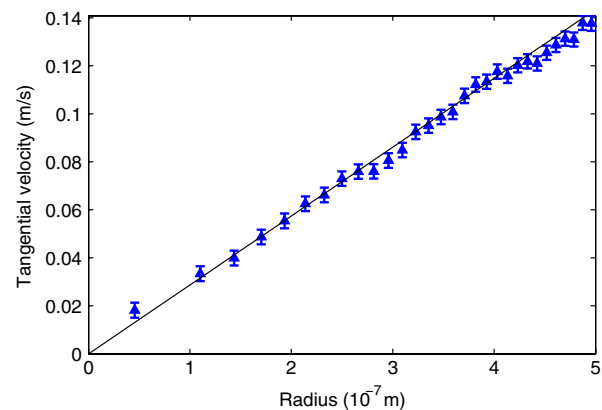

FIG. 3 (color online). Tangential velocity profile of the gas, which exhibits rigid-body-like rotation. The data are averaged over multiple DSMC runs, covering a time range of $t = 10^{-9}$–2×10^{-7} s. In this simulation, all the molecules initially rotate with an AM of $\langle J_z \rangle \sim 10\hbar$. The bars indicate the statistical error of our procedure. The solid line is a linear fit with $R^2 \sim 0.99$.

equation of state concluded the equation set. We used an axially symmetric finite-difference time-domain numerical scheme to solve the problem, with initial conditions based on the DSMC results. In order to prevent the edges of the simulation domain from affecting the central region we limited the simulation time. The full analysis of the numerical solution will be discussed elsewhere; here we report some of our observations.

Since the laser injects energy to the molecules by rotating them, the gas at the beam's focus is heated following the laser excitation. Figure 4(a) depicts the density crest the subsequent gas expansion creates. This density wave propagates outwards at about the speed of sound.

The radial profile of the directed tangential velocity shows a formation of a rigidly rotating core at the laser beam's focal spot [cf. Figs. 4(a) and 4(b)]. The profile exhibits a diffusionlike behavior in the radial direction. This phenomenon is attributed to the viscosity and is consistent with the notion of vorticity diffusion [23]. After the emerging acoustic wave had left the core, the temperature spreads diffusively, and so do the other thermodynamic and flow variables (cf. the density and vorticity radial profiles at several times in Fig. 4(c) and in the inset of Fig. 5, respectively).

At the postacoustic stage, the radial profiles of the velocity, density, pressure, and temperature at different times seem to become self similar. The source of the self similarity may be revealed by examining, say, the momentum conservation equation (tangential component):

$$\rho\left(\frac{\partial U_\theta}{\partial t} + U_r\frac{\partial U_\theta}{\partial r} + \frac{U_r U_\theta}{r}\right) = \mu\frac{\partial}{\partial r}\left(\frac{1}{r}\frac{\partial}{\partial r}(rU_\theta)\right), \quad (1)$$

where ρ, U_θ, U_r, μ, r, and t are the density, tangential and radial velocity, viscosity, radius, and time, respectively. The terms nonlinear in velocity on the left-hand side of Eq. (1) become comparable to the right-hand side of the same equation when the velocity components' magnitudes approach a characteristic velocity, $V_0 \sim \frac{\mu}{\rho w_0}$, with w_0 being the laser beam waist radius. For our simulated conditions, both radial and tangential velocities were small compared to V_0, making the second order velocity terms in Eq. (1) negligible. The relative density variations shown in Fig. 4(c) were less than 10%, and by taking a nearly constant viscosity, Eq. (1) reduces to a diffusion equation, known to have self-similar solutions. The "diffusion coefficient" is proportional to the kinematic viscosity $\nu = \frac{\mu}{\rho}$, and the characteristic diffusion time is $t_{\text{diff}} \sim \frac{w_0^2}{\nu} = \frac{w_0}{V_0}$. Following that insight, we found self-similar fits to the radial profiles of the gas parameters (after the acoustic wave has left the core). Specifically for the tangential velocity, Fig. 5 shows that the scaled calculated profiles converge with time to the Taylor vortex form [13,24]:

$$U_\theta(r,t) = \mathcal{H}\frac{w_0}{t_0}\left(\frac{t}{t_0}\right)^{-2}2\pi\left(\frac{r}{w_0}\right)e^{-(r/w_0)^2/(t/t_0)}; \quad (2)$$
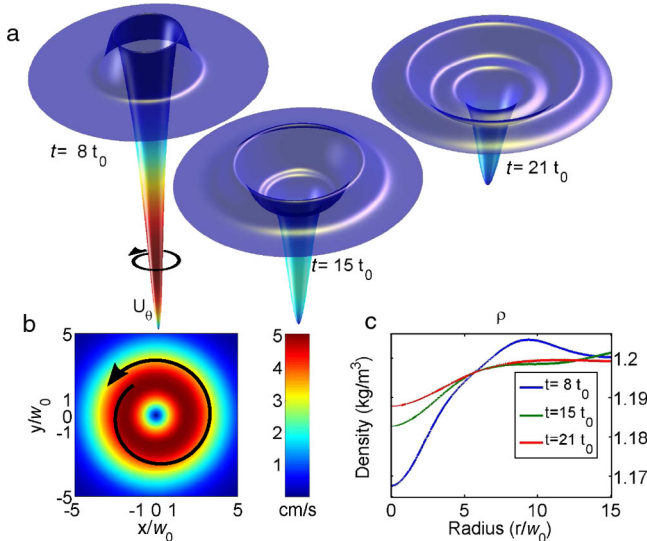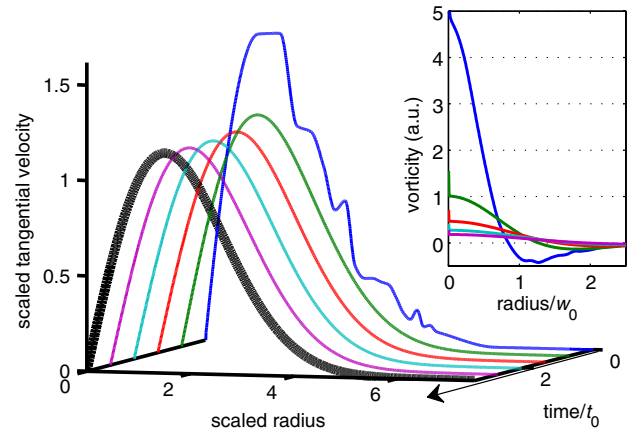

FIG. 4 (color online). (a) Spatial dependence of the gas density and the tangential velocity of the unidirectional rotation at different times. The time (from left to right) is $8t_0$, $15t_0$, and $21t_0$ after the simulation start [t_0 is the typical vortex time scale; see Eq. (3)]. The emerging acoustic wave is clearly visible, and the lower density core can also be noticed. The color coding represents the tangential velocity value, also shown in (b) in the plane perpendicular to the laser beam at $t = 8t_0$. The arrows in all panels indicate the rotation direction. (c) Density radial profile at the same times in the central region. The spatial coordinates throughout are in units of w_0, the radius of the beam's waist.

FIG. 5 (color online). Tangential velocity radial profiles at different times. The calculated tangential velocity U_θ is scaled as $U_\theta t^{3/2}\mathcal{H}^{-1}/[w_0 t_0^{1/2}]$; the radius r is scaled as $rt^{-1/2}/[w_0 t_0^{-1/2}]$. The plot shows a fast convergence to a self-similar Taylor vortex profile (thick black curve) given by Eqs. (2) and (3). The time t was offset by a vortex age [13] of $0.9t_0$ to produce the best fit. Inset: (unscaled) vorticity radial profiles at different times. The curves in the inset, from the highest to the lowest at the center, correspond to the five velocity profiles in the main graph, ordered by time. The radius here is in units of the laser beam waist w_0.

$$t_0 = \frac{w_0^2}{4\nu}, \qquad \mathcal{H} = \frac{\langle J_z \rangle}{8\pi m_{\mathrm{mol}}\nu}. \qquad (3)$$

The typical vortex lifetime, t_0, is in the order of t_{diff}, while the dimensionless vortex parameter, $\mathcal{H}$, depends on the average induced AM and characterizes the number of turnovers the core makes before the vortex viscous decay. $\langle J_z \rangle$ is the average of the axial component of the AM of the molecules excited by the laser and m_{mol} is the mass of the individual molecules. The Taylor solution [Eq. (2)] presents an expanding vortex structure having a finite total angular momentum. For a more elaborate treatment of self-similar vortices, see Ref. [25].

It follows from Eq. (2) that the rigid core of the vortex rotates at a frequency that drops with time as t^{-2}, while the typical core size grows as $t^{1/2}$. For a tightly focused laser beam ($w_0 \sim 1~\mu$m) that excites nitrogen molecules at atmospheric conditions to $\langle J_z \rangle \sim 100\hbar$, the vortex parameters are $\mathcal{H} \sim 10^{-2}$, $t_0 \sim 10^{-8}$ s. In this case a substantial initial rotation frequency of $\sim 10^5$ Hz may be achieved.

Consider now the motion of gas parcels as the vortex develops and decays. We calculated the parcels' trajectories both numerically and analytically with the help of Eq. (2), mapping each point to its location after the vortex had died. The jolt imparted by the laser excitation results in a finite angular displacement of the gas parcel. By repeating the excitation again and again the angular displacement accumulates, rotating parcels around the beam's axis as a "micro-torque gun," producing a motion similar to that of a ticking watch dial. At a pulse repetition rate of 1 kHz, the time interval between pulses is long enough for diffusion to wipe the temperature and density inhomogeneities and any radial displacement, even on a millimeter scale. Thus, in the micron-size waist of the laser beam only the azimuthal displacement grows from jolt to jolt. The video in the Supplemental Material [26] visualizes the angular displacement after many iterations. This angular displacement pattern may be experimentally observed by following the motion of micron-sized particles suspended in the whirling gas.

To conclude, we showed that laser pulses that induce unidirectional rotation of individual gas molecules produce a long-lasting macroscopic rotation of the gas. In a frictionless cylinder the gas reaches a steady rigid-body-like rotation. In free space a self-similar vortex forms and lasts significantly longer than both the pulse duration and the typical collision time. We also demonstrated that a repeated laser excitation can stir the gas in a pounding torque-gun motion accumulating to large angular displacement. The 100 kHz rotational motion of the gas vortex may be detected with the help of the rotational Doppler effect [27–29] or by usage of structured light spectroscopy [30]. According to our estimations the predicted collective spiraling motion is also observable by monitoring the motion of particles suspended in the gas. Finally, we emphasize that the appearance of the gas vortex is a direct manifestation of angular momentum conservation. In a sense, our laser induced effect presents a tabletop analogue to the formation of tropospheric cyclones, in which global rotational structures appear due to the inverse cascade scale up starting from the motion of turbulent eddies [31,32].

*uri.steinitz@weizmann.ac.il

[1] H. Stapelfeldt and T. Seideman, Rev. Mod. Phys. **75**, 543 (2003).

[2] B. Friedrich and D. Herschbach, Phys. Rev. Lett. **74**, 4623 (1995); J. Chem. Phys. **111**, 6157 (1999).

[3] J. Karczmarek, J. Wright, P. Corkum, and M. Ivanov, Phys. Rev. Lett. **82**, 3420 (1999).

[4] D. M. Villeneuve, S. A. Aseyev, P. Dietrich, M. Spanner, M. Y. Ivanov, and P. B. Corkum, Phys. Rev. Lett. **85**, 542 (2000).

[5] L. Yuan, S. W. Teitelbaum, A. Robinson, and A. S. Mullin, Proc. Natl. Acad. Sci. U.S.A. **108**, 6872 (2011).

[6] S. Fleischer, Y. Khodorkovsky, Y. Prior, and I. Sh. Averbukh, New J. Phys. **11**, 105039 (2009).

[7] K. Kitano, H. Hasegawa, and Y. Ohshima, Phys. Rev. Lett. **103**, 223002 (2009).

[8] S. Zhdanovich, A. A. Milner, C. Bloomquist, J. Floß, I. Sh. Averbukh, J. W. Hepburn, and V. Milner, Phys. Rev. Lett. **107**, 243004 (2011).

[9] J. P. Cryan, J. M. Glownia, D. W. Broege, Y. Ma, and P. H. Bucksbaum, Phys. Rev. X **1**, 011002 (2011).

[10] M. Lapert, S. Guérin, and D. Sugny, Phys. Rev. A **83**, 013403 (2011).

[11] F. Román, A. González, J. White, and S. Velasco, J. Chem. Phys. **118**, 7930 (2003).

[12] M. Uranagase, Phys. Rev. E **76**, 061111 (2007).

[13] G. I. Taylor, On the Dissipation of Eddies, Reports and Memoranda No. 598 (Brit. Advis. Comm. Aeronaut., 1918).

[14] G. A. Bird, *Molecular Gas Dynamics and the Direct Simulation of Gas Flows* (Clarendon, Oxford, 1994).

[15] P. Prasanth and J. Kakkassery, Fluid Dyn. Res. **40**, 233 (2008).

[16] K. Nanbu, Y. Watanabe, and S. Igarashi, J. Phys. Soc. Jpn. **57**, 2877 (1988).

[17] G. A. Bird, Phys. Fluids **30**, 364 (1987).

[18] M. P. Allen, D. Frenkel, and J. Talbot, Comput. Phys. Rep. **9**, 301 (1989).

[19] N. Hadjiconstantinou, A. Garcia, M. Bazant, and G. He, J. Comput. Phys. **187**, 274 (2003).

[20] C. Ngalande, S. Gimelshein, and M. Shneider, Phys. Fluids **19**, 128101 (2007).

[21] T. Colonius, S. K. Lele, and P. Moin, J. Fluid Mech. **230**, 45 (1991).

[22] M. Gad-el Hak, J. Fluids Eng. **117**, 3 (1995).

[23] S. I. Green, *Fluid Vortices*, Fluid Mechanics and its Applications, Vol. 30 (Kluwer Academic Publishers, Dordrecht; Boston, 1995).

[24] A. de Neufville, in *Fifth Midwestern Conference on Fluid Mechanics* (University of Michigan, Ann Arbor, MI, 1957), p. 365.

[25] F. Grasso and S. Pirozzoli, Phys. Fluids **11**, 1636 (1999).

[26] See Supplemental Material at http://link.aps.org/supplemental/10.1103/PhysRevLett.109.033001 for a video showing the accumulated displacement deformation of a virtual rectangular mesh as multiple vortex laser excitations are made. It spans over 15 000 iterations, exhibiting a substantial angular displacement. The coordinates are in units of the radius of the laser beam waist w_0; the vortex parameter is $\mathcal{H} \sim 10^{-4}$.

[27] B. A. Garetz, J. Opt. Soc. Am. **71**, 609 (1981).

[28] L. Allen, M. Babiker, and W. L. Power, Opt. Commun. **112**, 141 (1994).

[29] S. Barreiro, J. W. R. Tabosa, H. Failache, and A. Lezama, Phys. Rev. Lett. **97**, 113601 (2006).

[30] D. L. Andrews, *Structured Light and its Applications: an Introduction to Phase-Structured Beams and Nanoscale Optical Forces* (Academic Press, Amsterdam; Boston, 2008).

[31] E. Fedorovich, R. Rotunno, B. Stevens, and D. Lilly, *Atmospheric Turbulence and Mesoscale Meteorology*, edited by E. Fedorovich, R. Rotunno, and B. Stevens (Cambridge University Press, Cambridge, England, 2004).

[32] P. Tabeling, Phys. Rep. **362**, 1 (2002).